Pristine S,N-containing Mn-based metal organic framework nanorods enable efficient oxygen reduction electrocatalysis

Shujun Chao,*[a] Qingyun Xia,[a] Yingling Wang,[a] Wenge Li,[b] Wenge Chen[b]

[a] *Key Laboratory of Medical Molecular Probes, School of Basic Medical Sciences, Xinxiang Medial University, Xinxiang 453003, P. R. China*

[b] *School of Pharmacy, Xinxiang Medial University, Xinxiang 453003, P. R. China*

E-mail address: chaoshujun1979@163.com (S. Chao)

Tel: +86 373 3029128; fax: +86 373 3029128.

Supporting Information

Contents

Table S1. List of the ORR onset potentials (E_o) and half-wave potentials ($E_{1/2}$) of some reported MOFs.

Table S2. The Mn, O, C, N and S atomic percentages (%) of $Mn^{II}[(Tdc)(4,4'\text{-Bpy})]_n$, -1, -2, and -3 from XPS analysis.

Figure. S1 PXRD patterns (a) and N_2 sorption isotherms (b) of $Mn^{II}[(Tdc)(4,4'\text{-Bpy})]_n$-0 h, -2 h, -1, -2 and -3.

Figure. S2 N 1s and S 2p deconvolution spectra of $Mn^{II}[(Tdc)(4,4'\text{-Bpy})]_n$-1 (a and d), -2 (b and e), and -3 (c and f).

Figure. S3 (a) Polarization curves of Pt/C at different rotating speeds at 5 mV s^{-1}. (b) Koutecky-Levich (K-L) curves of Pt/C at 0.60, 0.55, 0.50, 0.45 and 0.40 V *vs*. RHE.

Figure. S4 PXRD patterns of $Mn^{II}[(Tdc)(4,4'\text{-Bpy})]_n$/C before and after the stability test for 20000 s.

For comparison, all the potential values from references were converted to *vs.* RHE in Table S1. All electrochemical tests were conducted in 0.1 M KOH solution.

Table S1. List of the ORR onset potentials (E_o) and half-wave potentials ($E_{1/2}$) of some reported MOFs.

Materials	E_o (V *vs.* RHE)	$E_{1/2}$ (V *vs.* RHE)	References
$Mn^{II}[(Tdc)(4,4'\text{-}Bpy)]_n$	0.98	0.78	This work
Mn/Fe-HIB-MOF	0.98	0.88	[1]
Mn-BTC@AC	0.92	0.78	[2]
Ni-Co-MOF	0.76	0.82	[3]
Ɛ-MnO_2/MOF(Fe)	0.84	0.64	[4]
Co/MIL-101(Cr)-R	0.95	0.67	[5]
rGO/(Ni^{2+}/THPP/Co^{2+}/THPP)$_8$	0.84	0.60	[6]

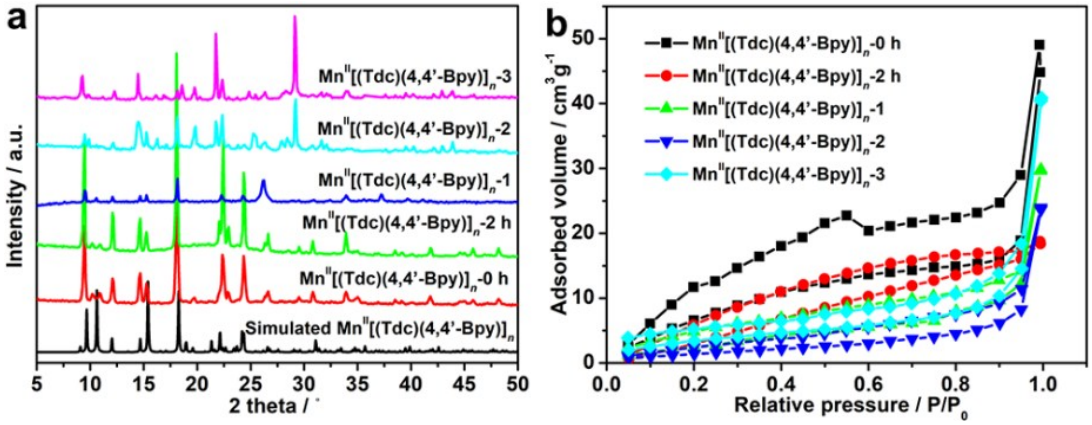

Figure. S1 PXRD patterns (a) and N_2 sorption isotherms (b) of $Mn^{II}[(Tdc)(4,4'\text{-}Bpy)]_n$-0 h, -2 h, -1, -2 and -3.

Table S2. The Mn, O, C, N and S atomic percentages (%) of $Mn^{II}[(Tdc)(4,4'\text{-}Bpy)]_n$, -1, -2, and -3 from XPS analysis.

Samples	Mn	O	C	N	S
$Mn^{II}[(Tdc)(4,4'\text{-}Bpy)]_n$	9.53	29.43	50.36	6.54	4.14

$Mn^{II}[(Tdc)(4,4'\text{-}Bpy)]_n$-1	6.63	24.64	58.89	5.71	4.08
$Mn^{II}[(Tdc)(4,4'\text{-}Bpy)]_n$-2	5.16	21.54	64.67	5.61	3.02
$Mn^{II}[(Tdc)(4,4'\text{-}Bpy)]_n$-3	14.43	40.52	39.08	3.8	2.17

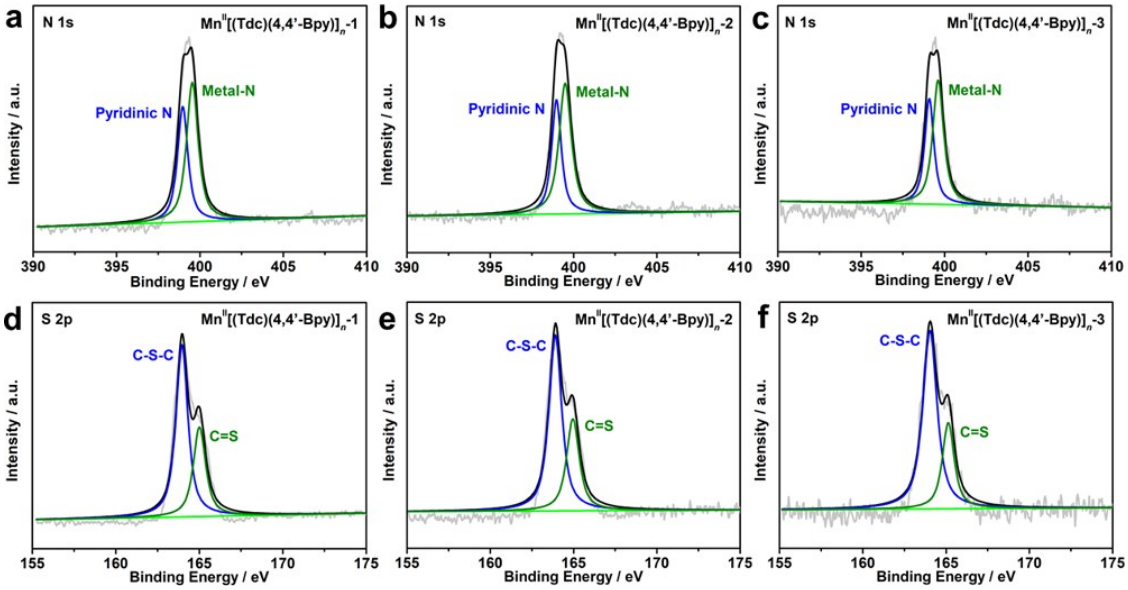

Figure. S2 N 1s and S 2p deconvolution spectra of $Mn^{II}[(Tdc)(4,4'\text{-}Bpy)]_n$-1 (a and d), -2 (b and e), and -3 (c and f).

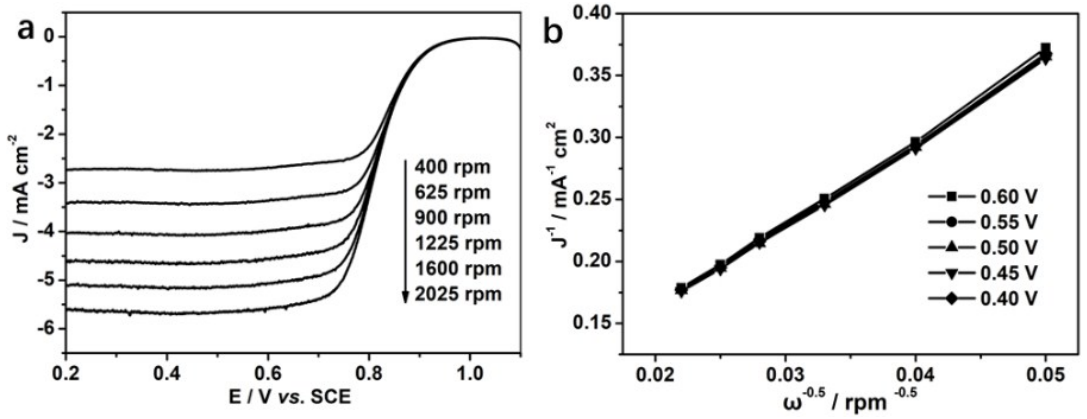

Figure. S3 (a) Polarization curves of Pt/C at different rotating speeds at 5 mV s^{-1}. (b) Koutecky-Levich (K-L) curves of Pt/C at 0.60, 0.55, 0.50, 0.45 and 0.40 V *vs*. RHE.

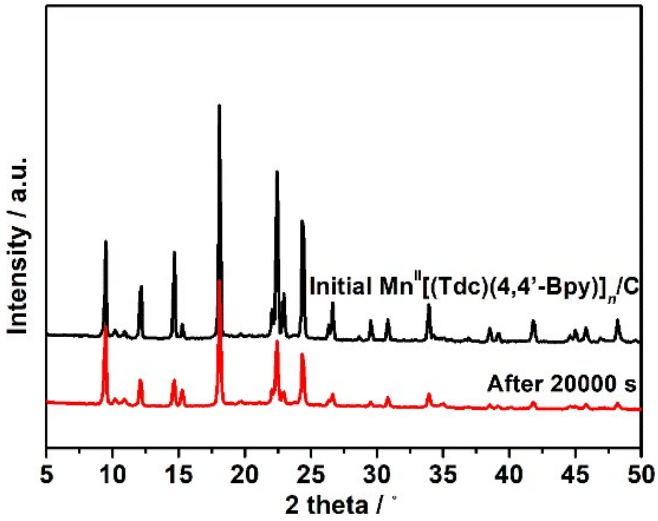

Figure. S4 PXRD patterns of $Mn^{II}[(Tdc)(4,4'\text{-}Bpy)]_n$/C before and after the stability test for 20000 s.

References

1 S. S. Shinde, C. H. Lee, J. Y. Jung, N. K. Wagh, S. H. Kim, D. H. Kim, C. Lin, S. U. Lee, J. H. Lee, Energy Environ. Sci., 2019, **12**, 727-738.

2 S. Gonen, O. Lori, G. Cohen-Taguri, L. Elbaz, Nanoscale, 2018, **10**, 9634-9641.

3 H. Xia, J. Zhang, Z. Yang, S. Guo, S. Guo, Q. Xu, Nano-Micro Lett., 2017, **9**, 43.

4 H. Wang, F. Yin, B. Chen, G. Li, J. Mater. Chem. A, 2015, **3**, 16168-16176.

5 X. He, F. Yin, G. Li, Inter. J. Hydrogen Energ., 2015, **40**, 9713-9722.

6 J. Sun, H. Yin, P. Liu, Y. Wang, X. Yao, Z. Tang, H. Zhao, Chem. Sci, 2016, **7**, 5640-5646.